WPBB-CPR(17) 17520

I Fernandez-Berceruelo et al.

Integration of the Neutral Beam Injector System into the DCLL breeding blanket for the EU DEMO

Preprint of Paper to be submitted for publication in Proceeding of 27th IEEE Symposium On Fusion Engineering (SOFE)

This work has been carried out within the framework of the EUROfusion Consortium and has received funding from the Euratom research and training programme 2014-2018 under grant agreement No 633053. The views and opinions expressed herein do not necessarily reflect those of the European Commission.

Integration of the Neutral Beam Injector System into the DCLL Breeding Blanket for the EU DEMO

I. Fernández-Berceruelo, D. Rapisarda, I. Palermo, F. R. Urgorri, P. Agostinetti, F. Cismondi, H. P.L. De-Esch and Á. Ibarra

***Abstract*—The integration of plant systems involving penetrations into the in-vessel components, like H&CD, fuel cycle and diagnostics, is a complex task constrained by top level requirements of remote maintainability and high reliability. Within the EUROfusion PPPT Program, some activities are ongoing to assess the integration of different systems into the breeding blanket, specifically NBI, ECRH launchers, diagnostics sightlines, fueling lines and specific protections for the FW (like start-up limiters).**

This work describes the integration of the Neutral Beam Injector (NBI) system into the Dual Coolant Lithium-Lead (DCLL) breeding blanket for the EU DEMO. After identifying the major issues impacting the mechanical, thermal-hydraulic and neutronic behavior of the blanket, the integration efforts have been focused on minimizing the invasiveness of the NBI system and exploring different NBI options for the best compromise between plasma heating and breeding blanket performance. This paper describes the adaptation of the DCLL breeding blanket design to allocate the neutral beam duct. A particular attention is devoted to the redistribution of breeding and shielding functions, the new path of fluid circuits and the additional cooling needs.

The consequences of design modifications on key neutronic aspects like Tritium Breeding Ratio (TBR) and shielding capability are addressed. Besides, the thermal loads transferred to the breeding blanket walls from the neutral beam and the plasma are discussed, and a preliminary thermal assessment of the proposed solution is presented.

***Index Terms*— Breeding Blanket, DEMO, Dual Coolant Lithium Lead (DCLL), Integration, Neutral Beam Injector (NBI)**

I. Fernández-Berceruelo, D. Rapisarda, I. Palermo, F. R. Urgorri and Á. Ibarra are with Laboratorio Nacional de Fusión, CIEMAT, Madrid 28040, Spain (e-mail: ivan.fernandez@ciemat.es; david.rapisarda@ciemat.es; iole.palermo@ciemat.es; fernando.roca@ciemat.es; angel.ibarra@ciemat.es).

P. Agostinetti is with Consorzio RFX, 35127 Padova, Italy (e-mail: piero.agostinetti@igi.cnr.it).

F. Cismondi is with EUROfusion Consortium, Power Plant Physics and Technology, 85748 Garching, Germany (e-mail: fabio.cismondi@euro-fusion.org).

H. P.L. De-Esch is with CEA-Cadarache, IRFM, F-13108 Saint-Paul-lez-Durance, France (e-mail: hubert.de-esch@cea.fr).

I. Introduction

THE integration in a fusion demonstration reactor of external systems which require penetrating the in-vessel components to reach the plasma chamber (heating and current drive, fuel cycle, diagnostics, etc.) is a difficult iterative process constrained by stringent requirements regarding reliability, remote maintainability and performance of the affected components.

Within the EUROfusion DEMO pre-conceptual design phase, some integration activities are ongoing in the framework of the Breeding Blanket Project (WPBB). The integration of ECRH launchers, diagnostics sightlines, fueling lines and specific protections for the first wall (i.e. start-up limiters) into the breeding blanket (BB) is being studied by different WPBB design teams. The integration of the Neutral Beam Injector (NBI) system into the BB is under investigation by the Dual Coolant Lithium-Lead (DCLL) design team. This work depicts the most critical NBI integration problems and proposes a preliminary design solution, especially focused on the issues linked to tritium production losses and heat loads.

II. Some Facts About the Design of the DCLL Breeding Blanket and the NBI System

The DCLL is one of the BB concepts under investigation within EUROfusion as a candidate for the European DEMO reactor. Although its design is being evolving within the course of the Project ([1], [2]), it is mainly characterized for working at low temperature (≤550 ºC) and it is based on the use of Pb15.7Li as breeder, main coolant, neutron multiplier and tritium carrier. Helium at 8 MPa is used to cool specific parts of the EUROFER structure.

The blanket follows the Multi-Module Segment arrangement, in which each segment is composed by a series of modules attached by bolts to a common Back Supporting Structure (BSS) (Figs. 1 and 2). The BSS integrates the service connections for all the modules and accomplishes shielding and supporting functions [3]. It includes a series of poloidal ducts covering the whole length of the segment which feed/recover the coolants to/from the modules. Inside the modules, the breeding zone is composed by several PbLi circuits (5-7, depending on the module) where the liquid metal flows in parallel mainly in poloidal direction (Fig. 3). The most updated mass flow and thermal gain corresponding to the outboard central segment (OBC) and its equatorial module (#4), respectively, are shown in Table I [4].

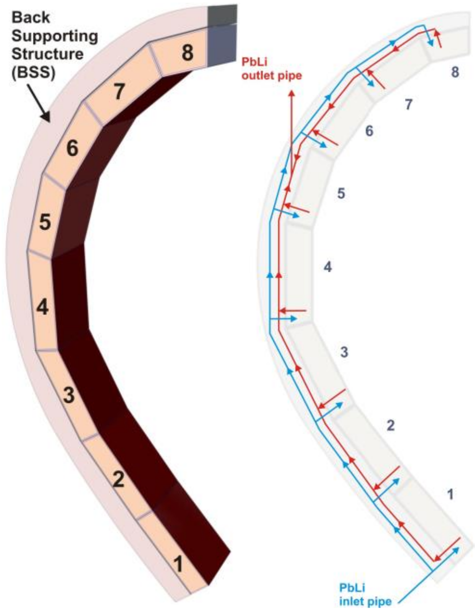

Fig. 1. DCLL outboard central segment (left). PbLi flow scheme (right).

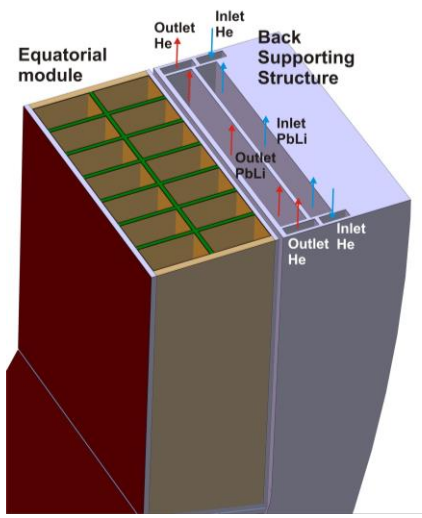

Fig. 2. Flow scheme in the Back Supporting Structure.

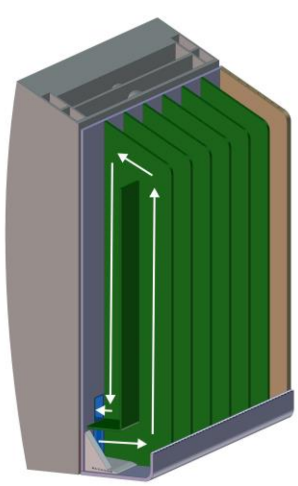

Fig. 3. PbLi flow scheme inside the OB equatorial module.

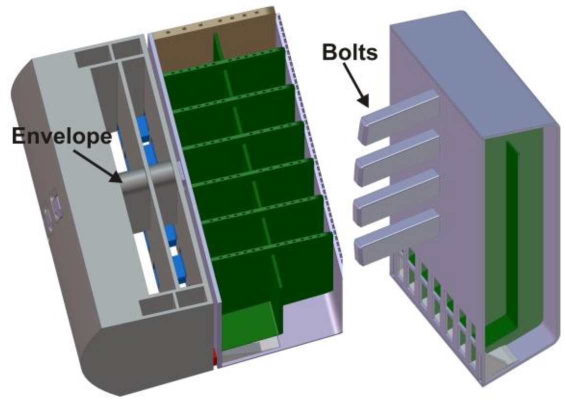

Fig. 4. Top view of the BSS and the OB equatorial module (top). Attachment system between the module and the BSS.

TABLE I
MASS FLOW, THERMAL GAIN AND DISTRIBUTION OF THE EXTRACTED POWER IN THE OBC SEGMENT AND THE EQUATORIAL MODULE [4].

	OBC module #4		OBC segment	
	PbLi	He	PbLi	He
Mass flow rate (kg/s)	52.87	1.56	393.4	11.95
Inlet temperature (ºC)	300	300	300	300
Outlet temperature (ºC)	550	465.2	547.3	452.4
Extracted power (%)	65.1	34.9	66	34

The design of NBI under development within EUROfusion is based on the “closed recirculating cavity with nonlinear gating” (RING) neutralizer concept. The RING concept features two lasers with 35 kW power and 1.5 nm wavelength (infrared), a second harmonic generator and a closed cavity mirroring system, composed of 6 upper mirrors, 6 lower mirrors and 4 mirrors with a 45º angle [5] [6]. This concept permits obtaining at the same time theoretical good neutralization efficiency and compact dimensions of the neutralizer. Indeed, in comparison with the ITER NBI, this design concept for the DEMO NBI could improve the injector overall efficiency from 26% to 51%, for an overall power released to the plasma around 50 MW [5] [6].

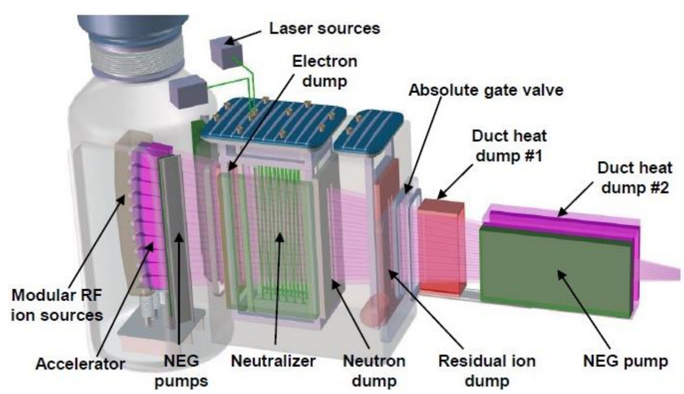

Fig. 5. Scheme of the NBI system (ref).

A key point for the NBI-BB interaction is the design of the duct, that is, the region which connects the beam line vessel to the plasma chamber going through the vacuum vessel (VV) and the BB. In the conceptual design of the DEMO NBI, a large non-evaporable getter (NEG) pump has been added to decrease the gas density in the duct and consequently the re-ionization heat losses, then minimizing the heat loads transferred to the BB [5] [6].

III. IDENTIFICATION OF MAJOR ISSUES

The opening of the duct through the BB can involve a series of issues linked to the removal of material with structural, breeding or shielding functions, the interception of fluids circuits and the interaction between the neutral beam and the blanket walls.

From the mechanical point of view, discontinuity in structural components, reduction of the section modulus, worse thermal/mechanical properties of the structural material because of higher radiation damage near the duct and additional difficulties for the remote maintenance strategy could be expected. From the thermal-hydraulic point of view, reduction of the channels cross-section area, modification of the fluids path, need of additional cooling circuits and additional difficulties to integrate thermal sources with different temperature ranges in the power conversion cycle are among the anticipated effects. Concerning neutronics, reduction of the tritium breeding ratio (TBR), lower capability to shield the toroidal field coils, neutron streaming along the penetration or shielding issues in the manifold/VV are likely to occur.

The impact of these potential issues strongly depends on which of the following scenarios take place:

1. If the system occupies a whole BB module the poloidal continuity of the BB modules could be jeopardized. This fact would compromise both the cooling system and the remote maintenance strategy.
2. If the system occupies only a part of the BB module the cooling system could be re-arranged, whereas the remote maintenance strategy should be probably different.

Considering the previous scenarios, the integration efforts have been focused on minimizing the invasiveness of the NBI system. Specifically, to avoid splitting the BB into two parts and to design the protection of the duct walls against heat loads from the beam and the plasma have been the main objectives.

IV. OPTIONS OF THE NBI FOR BETTER COMPATIBILITY WITH THE BLANKET

Two options for focusing the beam have been explored (Fig. 6): one on the tangential point of the plasma and the other on the center of the BB module. The best performance of the heating system would be achieved focusing the beam on the plasma (higher power concentration). However, this would oblige to enlarge the VV ports and to create a larger aperture in the blanket (near 2x1 m^2). The other option would originate a large beam section at the center of the plasma (lower power concentration), but would be better from the point of view of keeping the blanket functions, since the aperture in the BB would be smaller. Thus, it has been decided to adopt the second solution, at expenses of considerations from plasma physicists confirming this possibility.

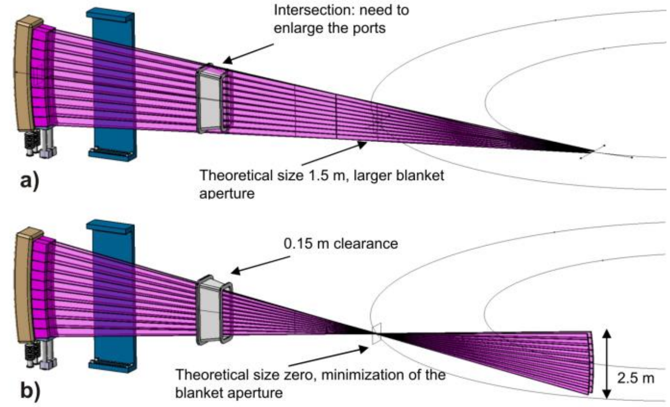

Fig. 6. Options for focusing the beam: a) at the middle of the blanket; b) at the tangential point of the plasma.

Another important point is the injection angle of the neutral beam, whose direction should be tangential to the plasma center for optimal momentum transference. Three different options [5] have been analyzed, where the angle of injection varies between 30 and 34.5º (Fig. 7). 34.5º corresponds to a situation where the beam enters tangentially to the plasma center, while 30º is the maximum angle which avoids the beam going through three OB segments, so that just two segments would be affected.

Together with the beam, the halo has to be considered. Therefore some clearance has to be respected. Thus, the explored possibilities for the size of the beam cross section (plus its halo) are 0.7 m x 0.7 m and 0.7 m x 1 m.

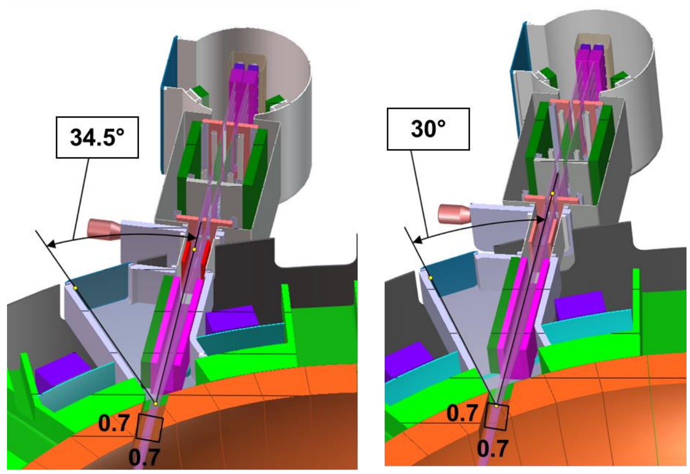

Fig. 7. NBI focalization on the center of the BB varying the injection angle and the cross-section area: options 1 (left) and 2 (right) [5].

The advantages of the option 1 (34.5º, 0.7 x 0.7 m^2) are the beam tangency at the center of the plasma and the minimization of the neutron fluence to the NBI, but it involves small clearance with the coils and the need of removing a small part of the VV. The option 3 (34.5º, 0.7 x 1 m^2) implies larger clearance around the beam, but this means higher neutron fluence to the NBI. On the other hand, the option 2 (30º, 0.7 x 0.7 m^2) ensures large clearance with the coils and does not need to remove part of the VV, although there is no beam tangency at the center of the plasma and higher neutron fluence to the NBI is expected.

Beam optics evaluations have showed that a clearance of 0.7 m x 0.7 m would be enough for focusing at the center of the blanket [5], and therefore this has been the selected option.

It is worth noting that the three possibilities only affect one entire module per segment, corresponding to the one located at the equatorial level. After some discussion the option 2 has been selected, because it affects only 2 segments while the other options could compromise also a third segment from the adjacent sector. This decision has a direct implication since the NBI is not tangential to the plasma center, and therefore this point has to be confirmed.

V. PROPOSED INTEGRATION SOLUTION

The assembly of the NBI and DCLL CAD models shows that the beam (including divergence) would affect both the BSS and the modules (Figs. 8 and 9). The beam intersects the breeding zone of just one module plus the corresponding BSS region of the lateral segment (OBL) and one side of the BSS of the OBC (Fig. 9). However, when the required clearance for the beam halo (0.7 m x 0.7 m) is considered the situation is more complicated since a small part of the breeding zone in the OBC is also affected (Fig. 10).

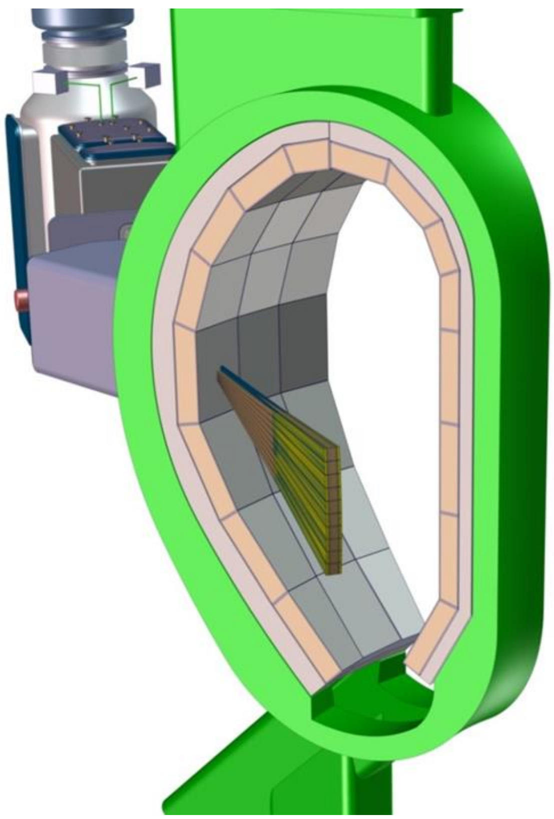

Fig. 8. Interference of the NBI system with the DCLL segments. General view.

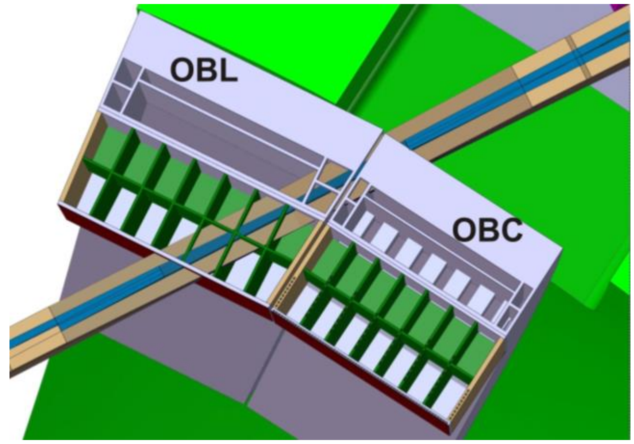

Fig. 9. Interference of the NBI system with the DCLL segments. Top view at the equatorial level.

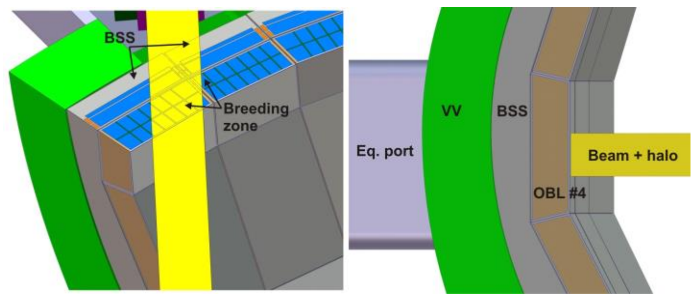

Fig. 10. Interference of the NBI system with the DCLL segments considering the beam and halo.

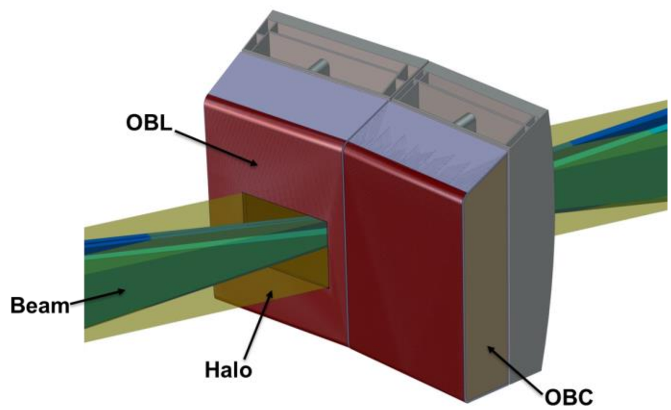

Fig. 11. View of the neutral beam + halo penetrating the BB modules.

In order to allow the beam going through the BB, a duct with the dimensions of the required clearance (0.7 m x 0.7 m) has been proposed (Fig. 11). The duct is shaped by different panels made of EUROFER, cooled by supercritical helium circulating through internal channels and covered by a tungsten layer of 2 mm thickness, similarly to the integrated first wall which is being considered in the DCLL [1]. The ideal solution would be a continuous duct crossing the blanket and guiding the beam. However, this is not possible because of the characteristics of the remote maintenance procedures (vertical extraction through the VV upper ports). In any case it would be difficult to integrate this continuous component between the segments. Thus, it has been decided to separate the duct into two parts corresponding to the OBL and the OBC segments. Fig. 12 shows the shape of the duct panels in both segments. The BSS is hidden in the bottom pictures to get a better view of both parts of the duct. Together with the duct, the bolts which attach the modules to the BSS can be observed.

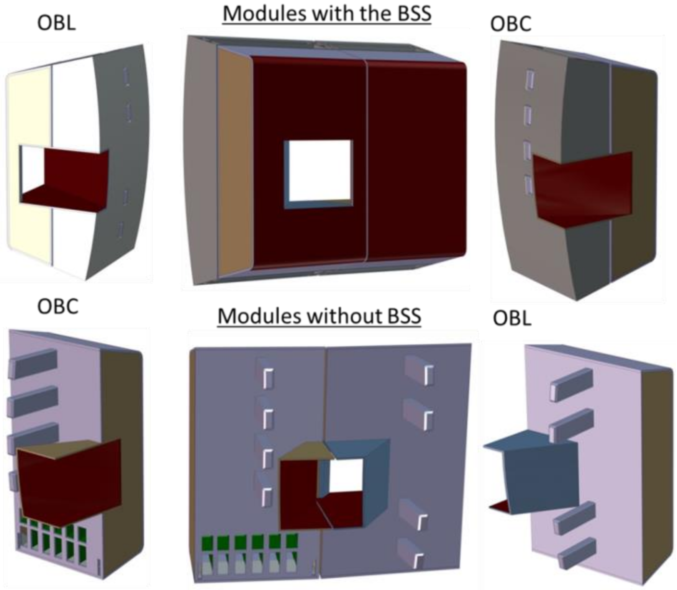

Fig. 12. Preliminary design of the duct to allow the penetration of the beam through the BB.

Fig. 12 clarifies that the duct has an important impact on the BSS of both segments. In particular, the cooling channels (PbLi and He) have to be re-arranged. The objective is to minimize the perturbations to the PbLi flow in the BSS, especially near the inlets/outlets to/from the modules (Fig. 13, in blue and red), where contractions, expansions and turns can implicate significant impacts on the flow. Thus, a trade-off between smooth and sinuous paths is required. The first ensure the flow is less disturbed, but the second allows keeping the He channels close to the external surface of the BSS, around the NBI duct, to counteract the effect of nuclear heating. The last approach has been followed in a conservative way for the thermal-hydraulic assessment of Section VIII (Figs. 13 and 14).

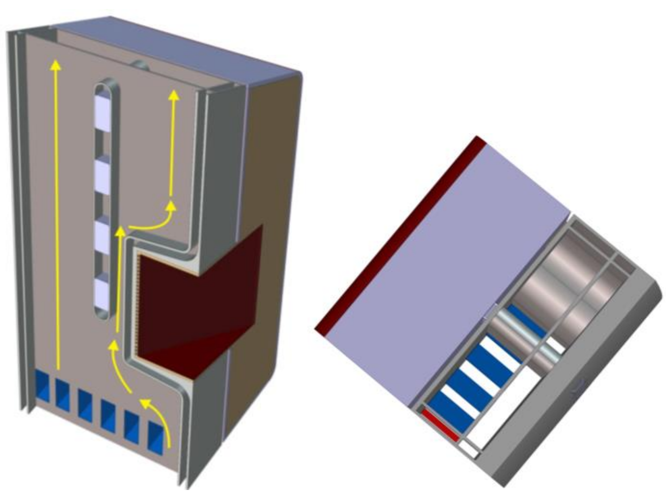

Fig. 13. Re-arrangement of the BSS PbLi and He circuits (OBC segment). In yellow, PbLi routing along the BSS inlet channel.

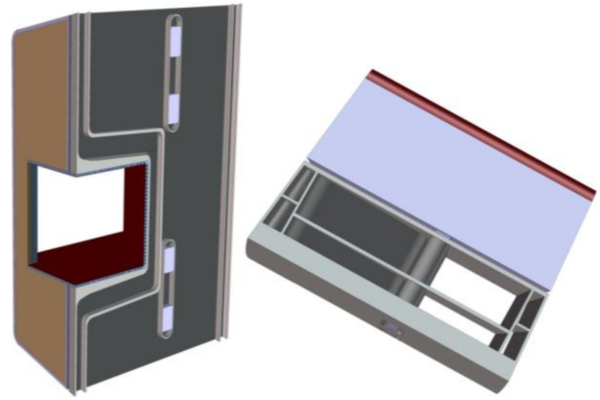

Fig. 14. Re-arrangement of the BSS PbLi and He circuits (OBL segment).

Regarding the affected parts of the breeding zones, in order to keep as much as possible the performance of the BB segments, different approaches have been considered to reduce the invasiveness of the NBI system, which is mainly translated into loss of breeding and shielding capabilities. Indeed, as a consequence of the duct opening, new areas of both the blanket and the BSS become exposed to the plasma. This can originate higher radiation heat flux and volumetric heat generation in the surrounding structures, higher neutron streaming to the VV and higher nuclear heating, fluence and damage in the toroidal field coils. Therefore additional shielding components with dog-legs paths/ labyrinths must be incorporated to reduce the direct irradiation from the plasma chamber.

Concerning the loss of breeding material (Figs. 9 and 10), the initial strategy was to split the OBL module in two smaller modules located above and below the duct, respectively, with the central volume took up by a shielding component. Nevertheless, the poloidal dimension of the resulting PbLi channels would be much reduced and the mass flow would be possibly unbalanced with the rest of modules. Taking it into account, it has been decided to adopt a simpler solution: 1) in the case of the OBL, the whole breeder function of the equatorial module is suppressed by filling the corresponding volume with shielding material such as steel, borated steel, tungsten carbide or metal hydrides (to be evaluated); 2) in the case of the OBC, just one PbLi circuit is suppressed by filling its volume with the same shielding material.

VI. EVALUATION OF THE TBR LOSS

The neutronic analysis of a half-sector of DEMO (10º) with the DCLL BB predicted a TBR value of 1.266 [7]. Table II presents a breakdown of the tritium production by type of segment and module (#1 is the outboard bottom module and #9 is the inboard top module, Fig. 1).

TABLE II
BREAKDOWN OF TRITIUM PRODUCTION BY SEGMENT AND MODULE [7].

Part	Module	10º sector		x360º
		OBL entire	OBC half	
	1	$1.45\cdot10^{-3}$	$9.97\cdot10^{-4}$	$8.81\cdot10^{-2}$
OB	2	$2.14\cdot10^{-3}$	$1.16\cdot10^{-3}$	$1.19\cdot10^{-1}$
	3	$2.70\cdot10^{-3}$	$1.25\cdot10^{-3}$	$1.42\cdot10^{-1}$

	4	$2.89\cdot10^{-3}$	$1.26\cdot10^{-3}$	$1.49\cdot10^{-1}$
	5	$2.07\cdot10^{-3}$	$9.29\cdot10^{-4}$	$1.08\cdot10^{-1}$
	6	$1.82\cdot10^{-3}$	$9.02\cdot10^{-4}$	$9.80\cdot10^{-2}$
	7	$1.44\cdot10^{-3}$	$8.49\cdot10^{-4}$	$8.25\cdot10^{-2}$
	8	$6.88\cdot10^{-4}$	$5.02\cdot10^{-4}$	$4.28\cdot10^{-2}$
IB	9	$1.34\cdot10^{-3}$		$4.81\cdot10^{-2}$
	10	$1.01\cdot10^{-3}$		$3.65\cdot10^{-2}$
	11	$6.78\cdot10^{-4}$		$2.44\cdot10^{-2}$
	12	$7.30\cdot10^{-4}$		$2.63\cdot10^{-2}$
	13	$1.38\cdot10^{-3}$		$4.98\cdot10^{-2}$
	14	$1.40\cdot10^{-3}$		$5.03\cdot10^{-2}$
	15	$1.26\cdot10^{-3}$		$4.52\cdot10^{-2}$
	16	$1.33\cdot10^{-3}$		$4.78\cdot10^{-2}$
Whole BB				1.158
BSS			OB BSS	$6.93\cdot10^{-2}$
			IB BSS	$3.92\cdot10^{-2}$
Whole BSS				$1.09\cdot10^{-1}$
Global TBR				1.266

According to the adopted configuration, the presence of 1 NBI system would imply the removal of one entire breeding zone (OBL #4), whose contribution to the local TBR is 0.00289, and one lateral PbLi circuit of the 7 which compose the OBC #4, whose contribution to the local TBR is 0.00252 (2x0.00126).

Considering the presence of 3 NBI systems in DEMO [5] [6], the final net TBR would be:

$$TBR_{NBI} = 1.266 - 3\cdot(0.00289 + 0.000359) = 1.256 \qquad (1)$$

This means that 0.769% of TBR loss is expected. If the breeder volume inside the BSS is also suppressed, a total loss less than 1% can be conservatively assumed. The target criterion of TBR = 1.1 [1] is widely fulfilled, so the decision of suppressing the breeding capability of OBL #4 and reducing the OBC #4 one is justified. In any case, a more comprehensive neutronic analysis from a specific model including the BB design adapted to the NBI system will allow a better characterization.

VII. EVALUATION OF THE SURFACE HEAT LOADS

One of the critical points in the integration of the NBI system into the blanket segments concerns the thermal loads acting on the surfaces of the duct panels which oblige including in the design a specific cooling system.

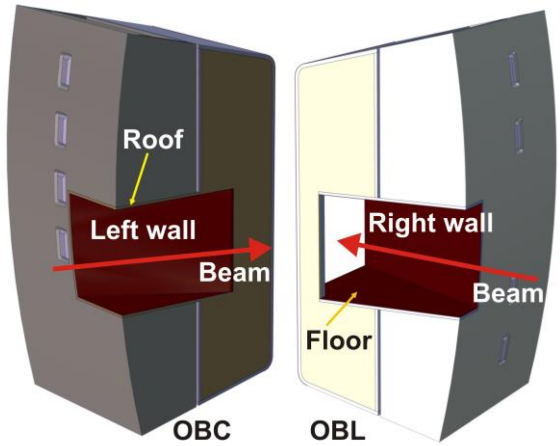

Fig. 15. Duct panels nomenclature.

Along the distance between the beam sources and the plasma (10.1 m length), and spite of the considered clearance, the neutral beam will transfer direct heat loads onto the surrounding components, including the BB walls. These loads correspond to both re-ionization of the beam due to the background gas that is present in the NBI duct and direct interception on the blanket walls. The produced ions will be deflected by the ambient magnetic field and hit the duct walls, thereby heating it.

The spatial deposition of neutrals on the duct panels has been calculated [8], finding that most of the power is actually transmitted to the roof and the floor of the duct, while the sides (left and right panels) receive very little power. This can be readily understood from the beamline design: top and bottom become narrow, whereas left and right widen. Thus, the neutral power to the roof and floor is the same and equal to 94 kW, due to symmetry, where the sides get 4 kW each [8].

In the case of re-ionized particles two cases must be distinguished: the start of flat top (SOF) and the end of flat top (EOF) of the DEMO pulses. For the BB integration, it has been decided to use the maximum values in order to cover the worst case (Table III).

Regarding the heat flux coming from the plasma, the considered peak radiation load is 500 kW/m^2 [1]. This value has been conservatively assumed for the surface of the 4 panels of the NBI duct in the BB. No heat loads coming from plasma particles have been included.

Table III summarizes all the heat loads used as inputs to design the cooling of the duct panels. The total heat flux on each panel has been determined by adding the heat loads from the beam uniformly distributed on the surface area to the heat flux from the plasma.

TABLE III
EVALUATION OF HEAT LOADS ON THE DUCT PANELS SURFACE

Heat loads from neutral beam [8]			
Plate	Beam direct interception (kW)	Re-ionized particles (SOF/EOF) (kW)	Total heat flux from beam (kW/m^2)
Left wall	4	(33/52)→ 52	75.88
Right wall	4	0	3.59

Roof	94	(22/4) → 22	107.11
Floor	94	0	89.44
Total	196	74	
	Heat loads from plasma		
	Radiation heat load (kW/m^2)	Particles heat load (kW/m^2)	Total heat flux (kW/m^2)
Left wall	500	-	575.9
Right wall	500	-	503.6
Roof	500	-	607.1
Floor	500	-	589.4

VIII. PRELIMINARY THERMAL-HYDRAULIC ASSESSMENT

The cooling scheme in the different panels of the duct has been defined following a similar approach than the used for the first wall of the DCLL [2], since the cooling requirements are similar. The configuration of helium channels shown in Fig. 16 (cross-section area of 15x10 mm^2 with 5 mm pitch) can withstand up to 600 kW/m^2 with reasonable helium velocities [9]. According to this scheme, a preliminary design of the channels arrangement in the different panels has been set (Fig. 17 and 18). In the case of the OBC module, the channels in the left, roof and floor panels can be fed from the side wall of the module, whereas the OBL module ones are more easily fed from the first wall circuit.

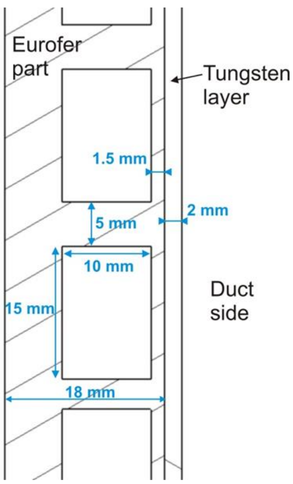

Fig. 16. Configuration of He channels.

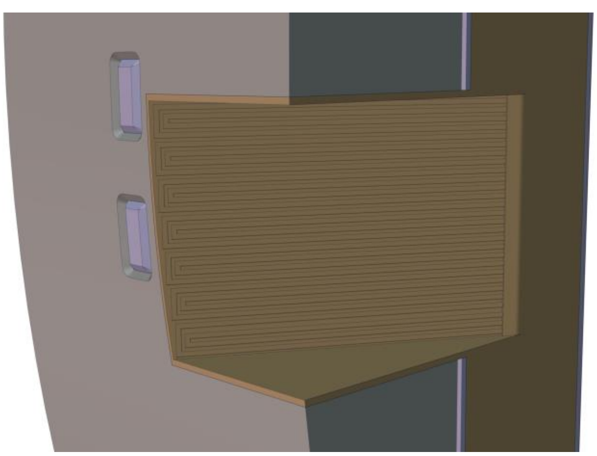

Fig. 17. Helium channels in the left panel.

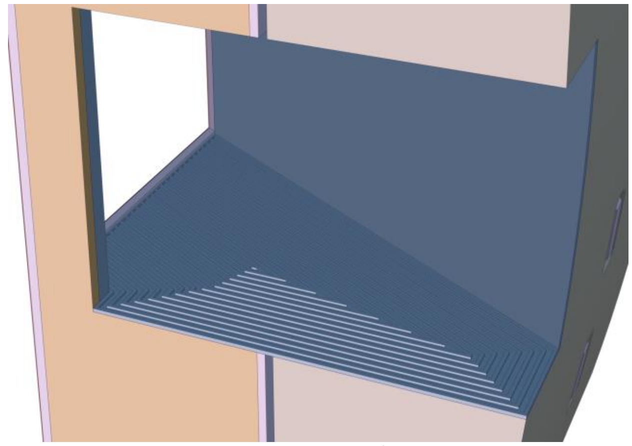

Fig. 18. Helium channels in the floor panel (OBL).

In order to evaluate the thermal behavior of the proposed solution, a steady-state thermal-hydraulic finite element analysis (FEA) has been carried out. The analysis employs coupled thermal-fluid pipe elements to represent the helium streams as fluid lines. Their nodes, with temperature and/or pressure as degrees-of-freedom, are connected to the solid elements through thermal surface effect elements. This approach supposes disregarding the diffusive heat transport inside the fluid, which is practically negligible in comparison with the convective one (high Péclet numbers), and assumes incompressible fully developed flow. It allows estimating the evolution of the fluid temperature along its path with enough accuracy, avoiding the need of performing computational fluid-dynamics analyses.

The problem is focused on the OBC module #4 and the model includes the corresponding section of the BSS, the back and left walls of the module, the attachments between the module and the BSS, the duct panels and the tungsten layer (Fig. 19).

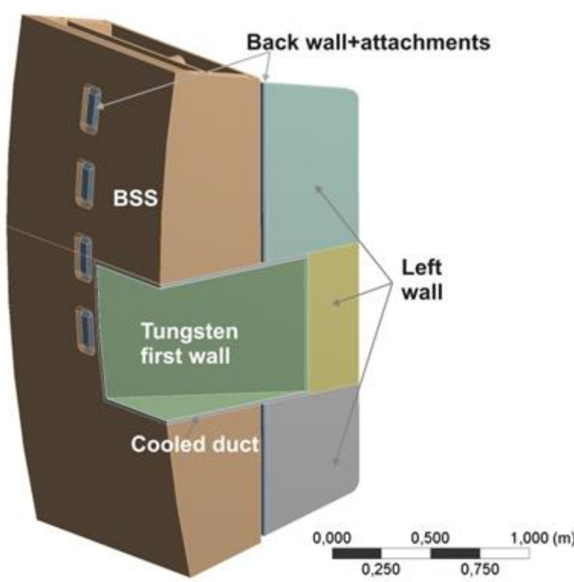

Fig. 19. Geometry model for FEA.

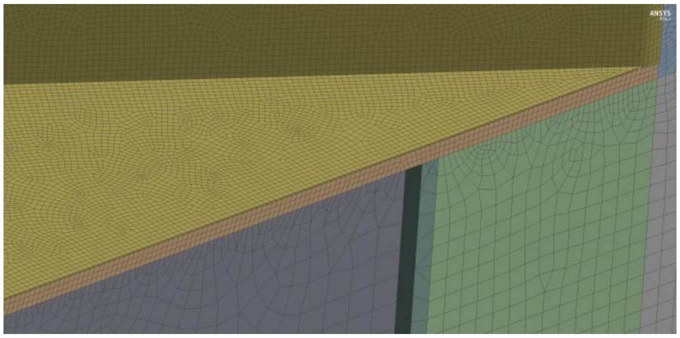

Fig. 20. Detail of the mesh.

The mesh, consisting of $2.3 \cdot 10^6$ nodes and $9.5 \cdot 10^5$ elements (Fig. 20), has been created in ANSYS Mechanical, whereas the rest of the preprocessing and the solving process have been carried out in ANSYS APDL.

With respect to loads and boundary conditions, heat fluxes have been applied on the surface of the tungsten layer (left, floor and roof), according to the values presented in Table III. Additionally, nuclear heating has been considered in the duct panels, the tungsten layer and the BSS. As a first approach uniform values of 3.96, 22.51 and 0.08 MW/m^3 have been respectively used. These numbers have been taken from [7] and, in the case of the panels and the tungsten layer, correspond to average values in the blanket first wall. Regarding materials, temperature-dependent properties have been defined for EUROFER, tungsten and helium (at 8 MPa).

Convective boundary conditions have been imposed on the walls of the BSS channels. The bulk temperatures and heat transfer coefficients (HTC) have been taken from the results of the PLATOON code [3]. Convective boundary conditions are also applied to the walls of the helium channels in the duct panels. Unlike in the BSS channels, the bulk temperature and HTC for each fluid or surface element have been calculated during the solving process by applying Gnielinski's and Ji&Gardner's correlations for He and PbLi, respectively [10] [11]. The He inlet velocity and temperature considered for the three panels circuits are respectively 75 m/s and 300ºC.

The resulting global temperature field in the BSS (Fig. 21) in clearly dominated by the convective boundary conditions on the BSS channels walls, which cause the apparition of two zones with significant differences in their average temperatures (310-550ºC for PbLi; 300-450ºC for He). The considered nuclear heating value for the whole BSS is not such a relevant heat source to counterbalance the cooling effect of the fluids flowing along the manifolds. This is particularly revealed in the case of the He channels, because of the lower bulk temperatures and higher HTC (~2800 W/m^2K vs ~500 W/m^2K in the case of PbLi). Returning to the issue of re-arranging the routing of the fluids in the BSS set out in Section V, this circumstance facilitates to modify the proposed path of the PbLi and He streams in order to smooth the profile of the flow expansions and contractions and, consequently, to reduce the pressure drop and the occurrence of flow separation.

The magnitude of the heat loads in the duct zone is mostly noted on the external surface of the tungsten layer, where the highest temperatures are achieved (539ºC). The performance of the helium circuits inside the EUROFER panels is enough to maintain their temperature under the limit of 550ºC. The highest temperature in the panels occurs at the interface with the tungsten layer in the roof panel (532ºC), where the heat flux from the neutral beam is maximum. In general, the combined effect of the duct cooling system and the flows in the manifolds allows maintaining the BSS temperature around the duct mostly below 400-450ºC. The peak temperature in the model (557ºC) occurs at the envelope of the bolts in the BSS hot PbLi channels (Fig. 4) but it is not related to the duct design and conditions.

From the mechanical point of view, the resulting temperature gradient in EUROFER can provoke the apparition of important thermal stresses that would be substantially aggravated by cyclic operation, like in the blanket first wall. Though, there is margin enough to increase the velocity of He and thus moderate the temperatures around the duct.

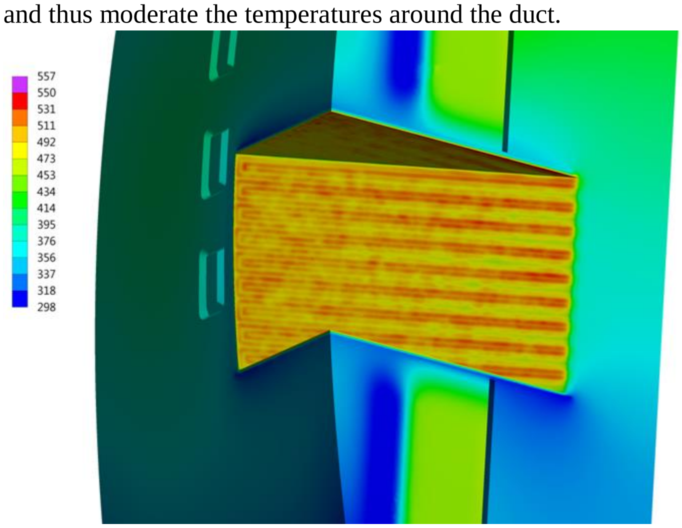

Fig. 21. Temperature field (ºC) around the duct.

With respect to helium, the average outlet temperature in the roof channels is slightly higher than in the floor channels, according to the higher heat flux (Table IV). However, the highest average outlet temperature corresponds to the left channels (361.5ºC). The reason is the larger average length of the left channels with respect to the other ones. The resulting average outlet temperature for the whole circuits (340.7ºC) is not high enough to be relevant for the power conversion cycle. Nevertheless, these streams can be connected in series to cool parts of the BB shielding modules subjected to moderate heat loads and, thus, to reach temperature ranges more suitable for thermoelectric conversion.

TABLE IV
HELIUM INLET AND OUTLET TEMPERATURES IN THE DIFFERENT CIRCUITS

Circuit	He inlet T (ºC)	Avg He outlet T (ºC)	Max He outlet T (ºC)
Left	300	361.5	365.1
Floor	300	325.7	349.9
Roof	300	329.0	356.0
Whole	300	340.7	365.1

IX. SUMMARY

The integration of the NBI system into the DCLL breeding blanket has been studied. The strategy has been focused on minimizing the impact on both systems. The adopted design solution consists in a duct which guides the beam through the blanket, affecting two BB OB segments. The duct is separated in two parts, shaped by EUROFER panels and covered by a tungsten layer. The panels are cooled by supercritical helium, in a way similar to the blanket first wall.

It has been decided to suppress or diminish the breeding capability of the modules affected by the duct, since the loss in the overall TBR can be lower than 1%, substituting the breeding material by shielding components. The preliminary layout of the duct panels and their cooling system is capable to protect the structure from the heat loads coming from the beam and the plasma, maintaining its temperature under 550ºC. Concluding, a solution has been found to keep the structural integrity of the segments, although this point must be confirmed by a comprehensive thermomechanical assessment. Also, a complete neutronic analysis of the proposed solution must be performed. It will provide actual nuclear loads and it will allow characterizing the shielding functions of the different shielding materials surrounding the penetration.

ACKNOWLEDGEMENTS

This work has been carried out within the framework of the EUROfusion Consortium and has received funding from the Euratom research and training program 2014-2018 under grant agreement No 633053. The views and opinions expressed herein do not necessarily reflect those of the European Commission. This work has been partially funded by the MEIC Ministry under Project ENE2013-43650-R.

REFERENCES

[1] D. Rapisarda, I. Fernandez, I. Palermo, M. Gonzalez, C. Moreno, E. Mas de les Valls, A. Ibarra, “Conceptual design of the EU-DEMO Dual Coolant Lithium Lead equatorial module”, IEEE Trans. Plasma Sci. 44-9 (2016) 1603-1612

[2] D. Rapisarda, I. Fernandez, I. Palermo, F.R. Urgorri, L. Maqueda, D. Alonso, T. Melichar, O. Frýbort, L. Vála, M. Gonzalez, P. Norajitra, H. Neuberger, A. Ibarra, “Status of the engineering activities carried out on the European DCLL”, Fusion Eng. Des. (2017), http://dx.doi.org/10.1016/j.fusengdes.2017.02.022

[3] I. Fernández-Berceruelo, D. Rapisarda, I. Palermo, L. Maqueda, D. Alonso, T. Melichar, O. Frýbort, L. Vála, Á. Ibarra, “Thermal-hydraulic design of a DCLL breeding blanket for the EU DEMO”, Fus. Eng. Des. (2017) http://dx.doi.org/10.1016/j.fusengdes.2017.03.108.

[4] I. Fernández-Berceruelo, I. Palermo, F. R. Urgorri, L. Maqueda, D. Alonso, J. Olalde, D. Rapisarda, “DCLL Design Report 2016”, EFDA_D_2MMM6Q, 2017.

[5] P. Sonato, P. Agostinetti, T. Bolzonella, F. Cismondi, U. Fantz, A. Fassina, T. Franke, I. Furno, C. Hopf, I. Jenkins, Conceptual design of the DEMO neutral beam injectors: main developments and R&D achievements, Nucl. Fusion 57 (2017) 056026.

[6] P. Sonato, P. Agostinetti, U. Fantz, T. Franke, I. Furno, A. Simonin and M. Q. Tran, Conceptual design of the beam source for the DEMO Neutral Beam Injectors, New J. Phys. 18 (2016) 125002.

[7] I. Palermo, D. Rapisarda, I. Fernández-Berceruelo and Á. Ibarra, “Optimization process for the design of the DCLL blanket for the European DEMOnstration fusion reactor according to its nuclear performances”, Nucl. Fusion, Volume 57, Number 7 (2017), 076011.

[8] H.P.L. De-Esch, “Re-ionised beam power in the DEMO duct”, EFDA_D_2MSR59, 2016.

[9] T. Melichar, O. Frýbort, L. Vála, P. Zácha, I. Fernández, David Rapisarda, “Optimization of the first wall helium cooling system of the European DCLL using CFD approach”, Fus. Eng. Des. (2017), https://doi.org/10.1016/j.fusengdes.2017.02.015

[10] V. Gnielinski, “New equations for heat and mass transfer in the turbulent pipe and channel flow”, Int. Chem. Eng. 16 (1976), 359-368.

[11] H. C. Ji and R. A. Gardner, “Numerical Analysis of turbulent pipe flow in a transverse magnetic field”, Int. J. Heat Mass Tran. 40 (1997), 1839-1851.